Food Chemistry: X 15 (2022) 100393

Contents lists available at ScienceDirect

Food Chemistry: X

journal homepage: www.sciencedirect.com/journal/food-chemistry-x

The effect of ion environment changes on retention protein behavior during whey ultrafiltration process

Wen-qiong Wang [a,d], Jian-ju Li [a], Ji-yang Zhou [a], Man-xi Song [a], Jia-cheng Wang [b], Xing Li [c], Cong-Cong Tang [e], Mao-lin Lu [a], Rui-xia Gu [a,*]

[a] College of Food Science and Engineering, Yangzhou University, Yangzhou 225127, Jiangsu, China
[b] Institute of Translational Medicine, Medical College, Yangzhou University, Yangzhou 225009, China
[c] School of Chemistry and Chemical Engineering, Harbin Institute of Technology, Harbin, Heilongjiang 150001, China
[d] Weiwei Food & Beverage Co., LTD, Xuzhou 221114, Jiangsu, China
[e] Shaanxi Key Laboratory of Environmental Engineering, School of Environmental and Municipal Engineering, Xi'an University of Architecture and Technology, Xi'an 710055, China

ARTICLE INFO

Keywords:
Whey protein
Ultrafiltration
Structural changes
Ion concentration

ABSTRACT

The factors affecting membrane fouling are very complex. In this study, the membrane fouling process was revealed from the perspective of ion environment changes, which affected the whey protein structure during ultrafiltration. It was found that the concentrations of Ca^{2+} and Na^{+} were overall increased and the concentrations of K^{+}, Mg^{2+} and Zn^{2+} were decreased at an ultrafiltration time of 11 min, which made more hydrophilic groups buried inside and increased the content of α-helix, leading to more protein aggregation. The relatively higher K^{+} ratio in retention could lead to an antiparallel β-sheet configuration, aspartic acid, glutamic acid and tryptophan increased, which resulted in more protein aggregation and deposition on the membrane surface at 17 min. When the ion concentration and ratio restored the balance and were close to the initial state in retention, the protein surface tension decreased, and the hydrophilic ability increased at 21–24 min.

Introduction

Recently, ultrafiltration technology has been widely studied to concentrate whey protein, but the relatively high production cost caused by membrane fouling in the ultrafiltration process restricts the promotion of membrane recovery of whey protein. The structural integrity of proteins is affected by the ultrafiltration process contributing to membrane fouling during filtration. When proteins penetrate membrane pores, they will be affected by external forces, such as tangential shear stress on the membrane surface and shear stress in the pore, resulting in changes in their structural characteristics (Portugal, Lima, & Crespo, 2008). Lactoglobulin (β-Lg), lactalbumin (α-La) and bovine serum albumin (BSA), as the main components of whey protein, all have spherical structures in their natural state, and show different melting spheres (MGs) and, monomer, oligomer and aggregation states according to the environmental conditions and processing technology. A large number of studies have analyzed the structural changes caused by protein adsorption to different materials and the effects of certain operating conditions, such as pressure, temperature, pH and ion environment, on the structure of the retention protein (Sethuraman & Belfort, 2005). In addition, the structural changes in proteins and the nature of the charge seem to be the main factors affecting membrane flux, and protein structure changes and charge effects could help explain the change in membrane flux. This result matched the changes in ion content and pH, and the results showed that ion content could cause changes in protein structure and play a favorable role in ultrafiltration (Van Audenhaege, Pezennec, & Gesan-Guiziou, 2013) (Table 1).

The common ions in the ultrafiltration process are mainly cations, such as Na^{+}, Ca^{2+}, Mg^{2+}, and K^{+}, Ca^{2+} has the ability to react with fouling molecules and the membrane surface, and their interaction changes the chemical properties of the membrane surface, forming network complexes with carboxyl compounds in fouling, making the gel layer of some macromolecules denser and more condensed, indirectly reducing membrane flux and causing membrane pollution (Ahn, Kalinichev, & Clark, 2008). In addition, Ca^{2+} bridges the ionic bridge between two adjacent carboxyl groups to form a complex through the bridging effect. Ca^{2+} bridging between adjacent BSA molecules can also increase membrane fouling. When the Ca^{2+} concentration is lower than

* Corresponding author at: College of Food Science and Engineering, Yangzhou University, Yangzhou 225127, Jiangsu, China.
E-mail addresses: jcw@yzu.edu.cn (J.-c. Wang), cctang0820@xauat.edu.cn (C.-C. Tang), lumlcn@yzu.edu.cn (M.-l. Lu), rxgu@yzu.edu.cn (R.-x. Gu).

https://doi.org/10.1016/j.fochx.2022.100393
Received 20 April 2022; Received in revised form 25 June 2022; Accepted 9 July 2022
Available online 16 July 2022

Table 1
Relative band intensities and assignments at selected regions of the Raman spectra of whey protein in retention during ultrafiltration process.

Main attribution	Wavenumber (Δcm^{-1})	Assignment
Tyrosine	850/830	State of phenolic OH group (exposed or buried, hydrogen-bond donor or acceptor)
Tryptophan	760, 880, 1360	Indole ring Sharp intense band indicates buried residues
Aspartic acid and glutamic acid	1400–1430	C═O stretch of COO–
	1700–1750	C═O stretch of COOH or COOR
	1450, 1465	C—H bending
	2800–3000	C—H stretching
Amide I (1600–1700)	1655 ± 5	C═O stretch, N—H wag ; α-Helix
	1670 ± 3	C═O stretch, N—H wag ; β-sheet
	1665–1685	C═O stretch, N—H wag
Amide III	1275	N—H in-plane bend, C—N stretch ; α-Helix
	1235 ± 5	N—H in-plane bend, C—N stretch ; β-sheet
	1245 ± 4	N—H in-plane bend, C—N stretch
β-sheet	1240	
SS	538	
Antiparallel β-sheet	1668	
RCOOH	1785	

1 mmol, the membrane flux is positively correlated with the Ca^{2+} concentration, and cake filtration is the main fouling model (Zhao, Yang, Li, Liang, & Hou, 2019). During ultrafiltration, ions in the solution environment can shield some impulse charges between adsorbed dirt molecules, resulting in increased adsorption (Tang et al., 2022). It has been found that increasing salt concentrations helps dissolve protein aggregates because the shielding of salt ions reduces the electrostatic attraction between protein molecules. DING et al. (Ding, Ma, Liu, & Qu, 2019) observed SEM images before and after ultrafiltration and the zeta potential of BSA at different Ca^{2+} concentrations, and found that the increase in Ca^{2+} concentration led to an increase in zeta potential, and Ca^{2+} shielded the surrounding charge, thus increasing the aggregation capacity of BSA molecules and the adsorption capacity on the membrane surface, intensifying membrane fouling. As hydration ions, Na^{+} and Mg^{2+} plasma produce hydration repulsion in the ultrafiltration process, which increases with increasing ionic strength. By reducing protein-protein interactions, Na^{+} and Mg^{2+} plasma promote their deposition on the membrane surface and form a loose and porous protein layer, which is conducive to increasing flux and delaying membrane fouling. In conclusion, the microscopic interaction behaviors of proteins at the ultrafiltration membrane interface under different ionic intensities showed that when the ion concentration reached a certain value, hydration repulsion would appear, which weakened the interaction between the ultrafiltration membrane and protein and thus led to the slowdown of the protein deposition rate and the reduction of membrane fouling (Kilmer, Huss, George, & Stennett, 2021). Mg^{2+} is one of the more abundant cations in general aqueous solution, and its relationship with membrane fouling behavior is similar to Ca^{2+}. When the Mg^{2+} concentration is low, the presence of both can enhance membrane fouling, which can be explained by the charge shielding effect, consistent with the theory of Derjaguin, Landau, Verwey and Overbeek (DLVO). When the concentrations of Mg^{2+} and Ca^{2+} increased, membrane fouling was significantly alleviated, but the alleviation mechanism of the two ions was different. For Mg^{2+}, hydration repulsion increased with increasing ion concentration, leading to an the increase in flux. Ca^{2+} was due to the stronger electrostatic repulsive force with protein molecules, which prevented intermolecular aggregation (Miao et al., 2017).

Ionic strength has been characterized by existing studies as a key factor affecting the membrane scaling rate in ultrafiltration. It plays an important role in protein structure and properties as well as protein-membrane and protein–protein interactions, so it has the possibility of improving the ultrafiltration process. Previous works have reported that protein structural and functional properties are altered due to ions with a functional (Fe^{3+} in the active center) and a structural function (Ca^{2+}) (Portugal, Lima, & Crespo, 2006). Classical DLVO theory provides a relatively clear explanation, which indicates that the scaling rate of protein increases with increasing ionic strength and will have a peak (Wang & Tang, 2011). However, some studies in recent years have shown that membrane fouling is significantly alleviated with increasing ionic strength during ultrafiltration. Some hydrated ions (such as Na^{+}) can adsorb negatively charged protein molecules, and the hydration repulsion generated increases with increasing ionic strength. The loose protein layer formed on the membrane surface delays membrane pollution, which is consistent with the pollution mechanism of filter cake filtration (Damar Huner & Gulec, 2017). When the ionic strength is high, the severity of film scaling is relatively mild, which may be because the protein solubility is also high at high salt concentrations. Therefore, the conformational change and higher solubility of protein molecules may be the reason why the decrease rate of membrane flux decreases with increasing ionic strength (She, Tang, Wang, & Zhang, 2009). In addition, SALGIN (Salgın, Takaç, & Özdamar, 2006) by cross-flow ultrafiltration experiments, also showed that with an increase in ionic strength and a compression of EDL leading to protein–protein and protein-membrane electrostatic interactions, a large number of proteins from the membrane surface are reduced, therefore, reducing the concentration of BSA on the surface of the membrane and improving the steady-state permeation flux of the membrane. In addition, the degree of ultrafiltration-induced protein denaturation depends on the pore size ratio of protein to membrane, as well as on permeation time and ionic strength, reflecting the potential effects that ions may play in protein ultrafiltration. The ionic environment in solution is one of the triggers for protein structural changes during ultrafiltration, and changes in these parameters also affect protein–protein and protein-membrane interactions. At present, there is no consistent explanation in all the studies and no clear theoretical knowledge to support further experimental research, but they have all stated that high ionic strength is helpful to alleviate membrane fouling. Therefore, more studies are needed to help us gain a deeper understanding of the linkages and influencing mechanisms between ion strength, protein structure and membrane fouling.

However, there are many kinds of ions in cheese whey solution, and the ion concentration varies over a wide range, so it is not clear how the ion concentration and the proportion of each ion influence the protein structure. The relationship between membrane fouling and protein structure changes is influenced by ion changes during the ultrafiltration process. Mastering the variation in protein structure with ion concentration during ultrafiltration has a positive impact on the control of membrane fouling. In recent years, research has mainly explored the mechanism of membrane fouling by observing the relationship between the change in single ions and membrane fouling. The aim of this study was to investigate the effects of ions on the protein structure and membrane fouling during the filtration process. The changes in protein structure with the ionic environment during the ultrafiltration process were studied to reveal the relationship between protein surface and secondary structure changes with the membrane fouling forming process. Then, the mechanism of membrane fouling was revealed from the perspective of the ion environment and protein structure changes.

Materials and methods

Materials

Polyethersulfone membrane (PES) with a molecular weight of 10 kDa was provided by Sepro (Nanostone Water. Co., Chicago, USA). Whey is extracted from our laboratory production of cheddar cheese.

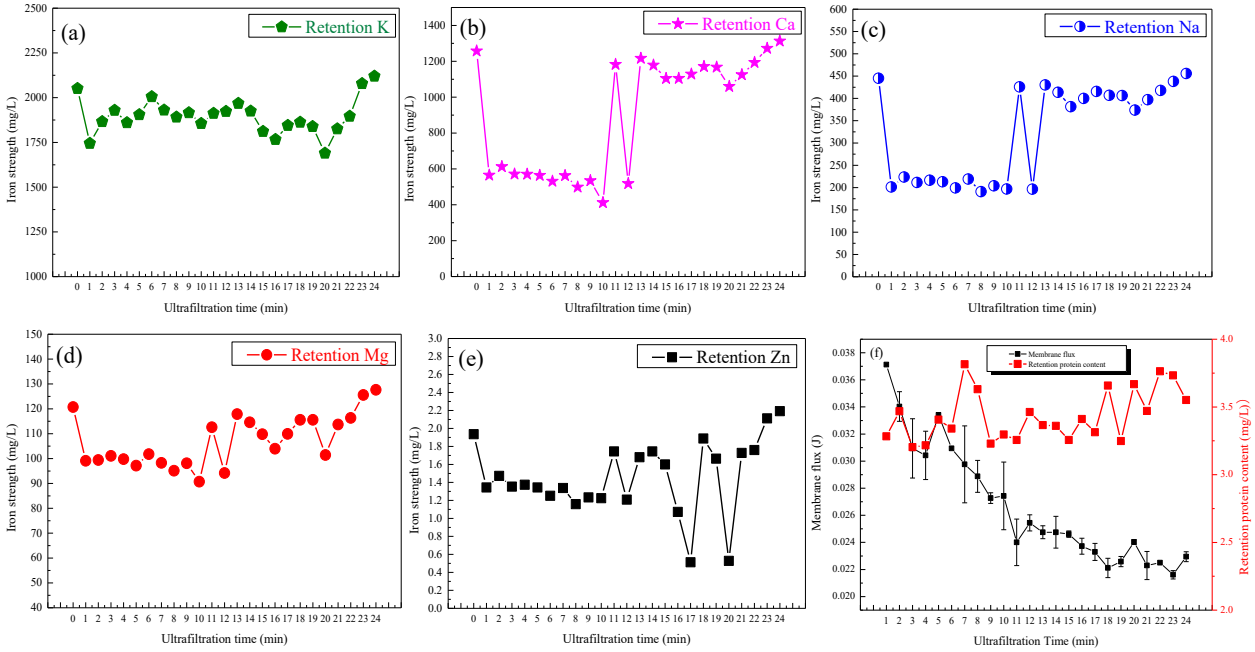

Fig. 1. The ion strength (K^+, Ca^{2+}, Na^+, Mg^{2+}, Zn^{2+}) changes of retention during whey ultrafiltration process (a–e). The whey protein content in retention and membrane flux changes (f) during ultrafiltration process.

Methods

Whey protein content of the retention fluid

We added 50 mL of sample to an ultrafiltration cup for each experiment. The transmembrane pressure was set at 0.15 MPa. Finally, the content of retention protein was determined by the Lowry protein assay method (Wen-qiong, Lan-wei, Xue, & Yi, 2017).

Membrane flux measurements

The ultrafiltration performance of whey protein was characterized by a dead-end filtration system at a transmembrane pressure of 0.15 MPa. The membrane permeability flux was calculated by the following formula:

$$J = \frac{V}{A\Delta t} \quad \text{Relative flux} = J/J_0$$

In the formula, A (cm^{-1}) is the membrane surface area, V (ml) is the volume of permeable liquid under different ultrafiltration times, Δt (min) is the time change between two mass measurements, and J_0 is the pure water flux of the membrane (Miller, Kasemset, Wang, Paul, & Freeman, 2014). The concentration efficiency of whey protein in different ionic environments was measured.

Flame atomic absorption spectroscopy

The metal content was determined by a PinAAcle 900F atomic absorption spectrometer (United States, PerkinElmer). A hollow cathode lamp and deuterium background corrector were used at their respective wavelengths, and an air-acetylene flame was used. The lamp currents of K^+, Mg^{2+}, Na^+, Ca^{2+} and Zn^{2+} were 8, 10, 8, 12 and 6 mA, respectively (Klost, Giménez-Ribes, & Drusch, 2020).

Particle size distribution

The particle size distribution of the samples was determined by a Zetasizer Nano ZS (Malvern Instruments). Scattered light detection was performed at a 173° angle with laser attenuation. The measuring position was determined by Malvern software automatic adjustment.

Zeta potential measurements

At 25 ± 0.1 °C, the zeta potential was used to analyze the charge changes of the protein polymer surfaces. Zeta potential was measured using a Malvern Zetasizer Nano ZS (Brookhaven Instruments, USA).

Surface tension measurement

In this experiment, a K100 tensiometer from Germany KRUSS Co. was used for testing. The surface tension of the protein solution was measured by the hanging sheet method. The sample cup of the surface tensiometer moves along the sample table and the solution to be tested in it is in contact with the standard hanging plate. A change in force occurs at the surface contact point. The surface tension of the solution to be measured can be calculated by measuring the mass change value of the standard sheet on the surface (Adhikari, Howes, Shrestha, & Bhandari, 2007).

FTIR

FTIR spectra were recorded according to a prior method with some modifications (Dineshbhai et al., 2022). FTIR spectra were recorded in ATR mode on a Varian Cary 610/670 FTIR spectrometer (Varian, Salt Lake City, NV, USA), using the Turbo mode of the Ever Glo infrared source. All samples were measured after freeze-drying. The temperature of the sample was kept at 25.0 ± 1.0 °C with the aid of an external Specac West 6100 + controller. The resolution was 4 cm^{-1}, and the wavelength range was 400 to 2200 cm^{-1}. Using loading pressure, the sample was placed near the diamond crystal.

Determination of Raman spectra

The membrane surface proteins were dispersed into a 100 mg/ml solution in pure water, stored at 5 °C for 48 h, and then analyzed after complete H/D exchange. Experimental conditions included a scanning frequency range of 200–1800 cm^{-1}, 632.8 nm wavelength, He-Ne laser, integral time of 100 s, 6.4-mW power, and room temperature (Wagner, Biliaderis, & Moschakis, 2020).

Statistical analysis

Experimental data were statistically analyzed using SPSS 11.5 software (SPSS, Inc., Chicago, IL). One-way ANOVAs were applied to examine the effects of different treatments. Data are expressed as the means ± standard deviation. Duncan's multiple range tests were

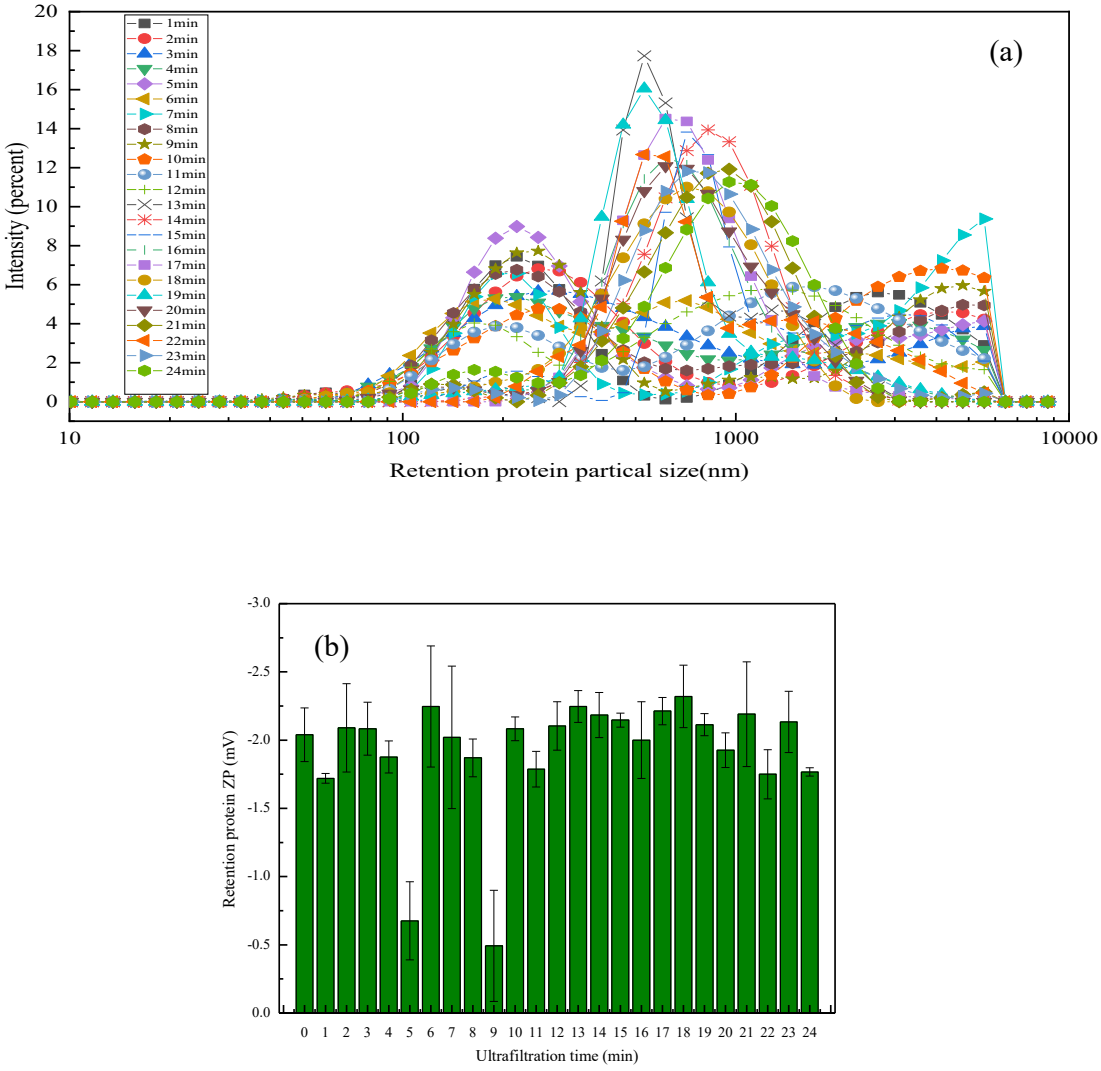

Fig. 2. Particle size analysis (a) and Zeta potential analysis (b) of retention protein during ultrafiltration of whey protein.

performed for post hoc multiple comparisons with the level of significance set at $P < 0.05$.

Results and discussion

The ion strength and content of retention protein during ultrafiltration with membrane flux changes

The membrane flux is related to the content of retention proteins. In the absence of salt ions, the maximum retention occurs at the isoelectric point, but it is larger in the presence of salt ions. The results explain the influence of different ion environments on protein permeability. Ions with the same charge have different effects on the solubility of proteins in water, and the unique effect of different ions on the stability of proteins in solution is considered the Hofmeister effect. This effect cannot be considered simply as affecting the solubility of a protein, but also requires analysis of how ions interact with the protein, as well as hydration leading to changes in protein stability and aggregation (Moghaddam & Hormann, 2019). It has been suggested that structural changes and higher solubility of proteins may be responsible for the decrease in membrane flux rate with increasing ionic strength. The contamination rate of protein increases with increasing ionic strength, and peaks occur (Gao et al., 2018). As shown in Fig. 1, the ion content of Ca^{2+} and Na^{+} in the retention liquid decreased significantly and rose sharply after 12 min, while the ion contents of Mg^{2+}, Zn^{2+} and K^{+} changed slightly at the initial stage of ultrafiltration and showed a fluctuating trend after 10 min. At the same time, the ion content of K^{+} is obviously higher than that of other ions. After 5 min during the ultrafiltration process, the ion content of K^{+} increased, the membrane flux increased, and the protein content in the retention liquid increased. At this time, Ca^{2+} did not change significantly, and the insoluble calcium salt was not formed. At 7 min, the contents of Ca^{2+}, Na^{+} and Zn^{2+} in the retention liquid increased slightly. As shown in Figs. 1 and 2, the content of retention protein and membrane flux decreased. Ca^{2+} can enhance membrane fouling by binding to adjacent proteins and reducing their charge. Through the bridging effect, two adjacent carboxyl groups are connected to form ion bridges and BSA-Ca complexes. At 12 min, the contents of Ca^{2+}, Na^{+}, Mg^{2+} and Zn^{2+} in the retention liquid decreased sharply, while the contents of retention protein increased, possibly due to the ion exchange effect. A reversible exchange occurs between cations or anions in the ionic environment and isotropic ions in solution. On the other hand, the interaction between ions and organic matter changes the size and structure of organic matter, and promotes the aggregation of pollutants through complexation with organic matter. Therefore, theoretically, the structural changes of organic matter caused by the coexistence of multiple ions will have a significant impact on the retention and membrane fouling of organic matter. The contents of all ions increased and gradually peaked after 20 min, and the contents of

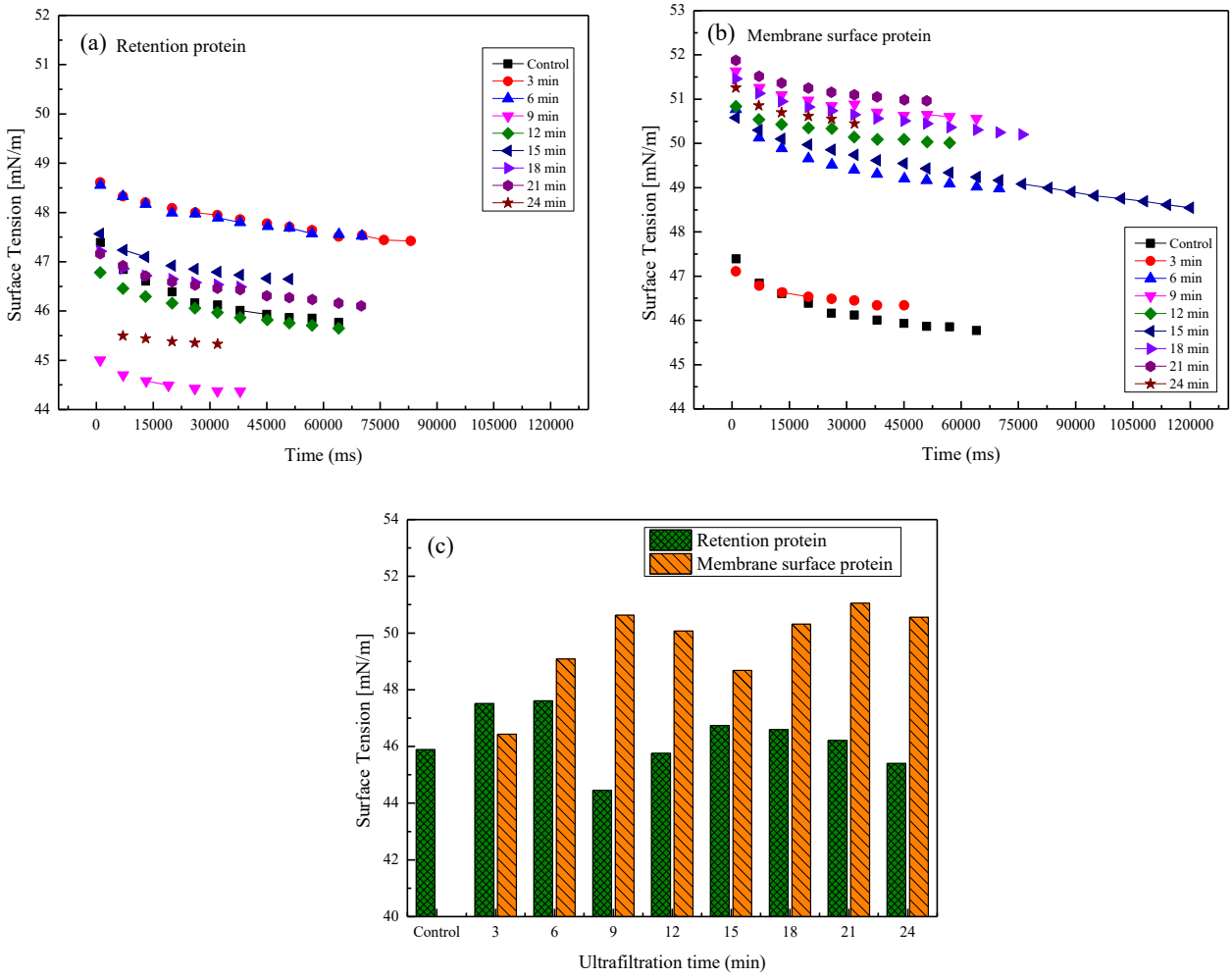

Fig.3. Surface tension (mN/m) changes of retention (a) and membrane surface (b) during ultrafiltration of whey protein.

retention protein and membrane flux showed an upward trend after a slight decrease. This indicates that when the ion content is close to the initial value of the process, it is beneficial to the recovery of the membrane flux.

The change in concentration efficiency and fouling of protein on the membrane surface can be observed by the change in retention protein content. As shown in Fig. 1(f), with the extension of ultrafiltration time, the content of retention proteins showed a fluctuating upward trend, which was because some of the membrane surface proteins are transferred to the retention liquid during the ultrafiltration process. The interaction between proteins and the membrane is affected by many factors, so it is necessary to ensure that the structural integrity of proteins is not affected during the ultrafiltration process to prevent the changes in protein structure from exacerbating membrane fouling. Therefore, not only membrane flux and protein concentration efficiency, but also protein structure and biological activity should be considered when optimizing the operating conditions. When the transmembrane pressure remained constant, the change in protein surface structure was attributed to the change in ion concentration with the change in ultrafiltration time. As shown in Fig. 1(f), the retention protein increased sharply at 6 min, indicating that some of the proteins on the membrane surface were washed away and entered the retention liquid. However, when the ultrafiltration times were 2, 7, 12 and 18 min, this decreased slightly, which may be because some ions played a role in cross-linking, enhancing the protein–protein interactions. The protein content decreased slightly at 10 min, which was related to the increase in Na^{+} and Mg^{2+}, as shown in Fig. 1(a) and (d). As hydration ions, they generate hydration repulsion during ultrafiltration. By reducing protein–protein interactions, they promote deposition on the membrane surface and form loose and porous protein layers, which is conducive to increasing flux and delaying membrane fouling. At 18 min, the retention protein content increased because the density of the sediment layer increased with the filtration time, and the exposure of hydrophobic groups increased protein aggregation, enhanced protein cross-linking, and caused protein accumulation on the membrane surface to form a filter cake layer.

Optimization of the ultrafiltration membrane process and permeation flux has been the focus of most studies, but the ultrafiltration time, temperature, pH, pressure, ion environment and other factors can affect the membrane flux. As shown in Fig. 2, membrane flux is negatively correlated with ultrafiltration time, which decreases with time. The increase in flux at 5 and 20 min may be related to the increase in retention protein content, and the membrane surface protein was washed into the retention liquid, resulting in a decrease in the force between the protein and membrane. After 14, 18 and 22 min, the membrane flux increased due to the hydration of Na^{+} and Mg^{2+}. In addition, the decrease in membrane flux at 21 min can be attributed to the formation of reticulated complexes between Ca^{2+} and macromolecule carboxyl compounds, which causes them to form a relatively dense fouling layer structure on the membrane surface, thus reducing the membrane flux. However, at the later stage of the ultrafiltration process, the ion concentration is high, which can shield some impulse charges between adsorption molecules, resulting in increased protein adsorption and reduced membrane flux (Rui et al., 2015).

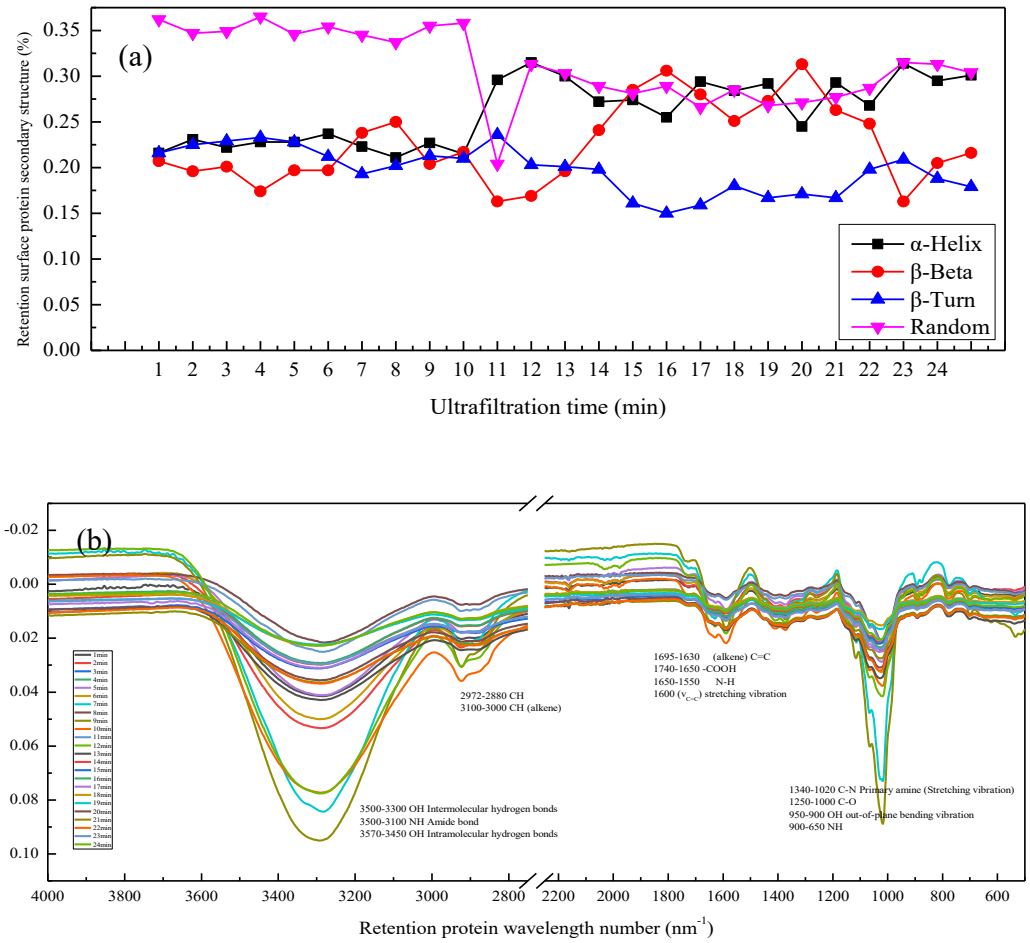

Fig. 4. The secondary structure changes (a) and FTIR analysis (b) of whey protein in retention during ultrafiltration process.

Particle size and zeta potential of retention protein during ultrafiltration

The particle size distribution of whey protein at different ultrafiltration times was investigated. During this process, polymerization occurred between proteins, and larger particles of protein rapidly deposited on the membrane surface. Only under specific conditions can the appropriate size of aggregates improve the membrane flux (Zhang et al., 2022). As shown in Fig. 2(a), some of the particle sizes increased after 10 min, which indicated that ion changes could cause protein aggregation. This could lead to loose cake resistance on the membrane surface, which may come into retention at some times and reduce membrane fouling. However, this condition lasted for a short time. Then, all the particle sizes were increased after 12 min. The amount of protein surface charge has a certain influence on the filtration effect and stability of the filtration system, especially the concentration polarization. When Zeta is negative, the greater the absolute value is, the better the stability of the system. In the concentrated polarization layer, the deposition of whey protein on the membrane is mainly controlled by the electrostatic repulsion force (Rohani & Zydney, 2010). However, the zeta potential of the protein surface after 12 min fluctuated slightly compared to that at 0 min (at filtration beginning), which indicated that the zeta potential of protein surface changes was slight after 12 min. This also indicated that the protein surface's zeta potential had a slight effect on protein aggregation during the filtration process. Therefore, the protein aggregation was related to the groups on the protein surface changes after filtration for 12 min, which also led to the formation of hard protein cake resistance. Furthermore, the resistance was irreversible for long-term membrane operation.

Surface tension of the retention protein during ultrafiltration

The surface tension is related to the polarity of the liquid, the size of the molecules in solution, the interaction force between the molecules in the liquid, and so on. As shown in Fig. 3, the protein surface tension was investigated for the protein in retention and membrane surface to compare the protein changes during the ultrafiltration process. It was found that surface roughness, the yield stress of the sample and solid surface tension were the key factors responsible for adhesion (Adhikari et al., 2007). As shown in Fig. 3, the surface tension for membrane surface proteins was higher than that for retention proteins, which indicated the exposure of some hydrophobic fragments, previously buried inside (partial unfolding) (Wojciechowski, 2022). This is why the whey protein on membrane surface changed from loose cake to hard cake protein resistance. On the one hand, the protein surface tension in the retention was increased after 9 min. On the other hand, the surface tension of protein on the membrane surface was also increased with the ion concentration and proportion changes. However, the protein surface tension was decreased after 21 min for retention and the membrane surface protein, as shown in Fig. 3. This was related to the ion concentration and ratio return to initial state the (0 min), as shown in Fig. 1. This means that with the right concentration and ratio of ions, the protein's surface tension can be restored to its original state. Although the ion environment was good for whey protein retention, a hard protein cake formed. Therefore, the flux was still reduced, and membrane fouling formed. Therefore, the ion ratio and concentration in the feed had a considerable effect on protein structure and membrane fouling.

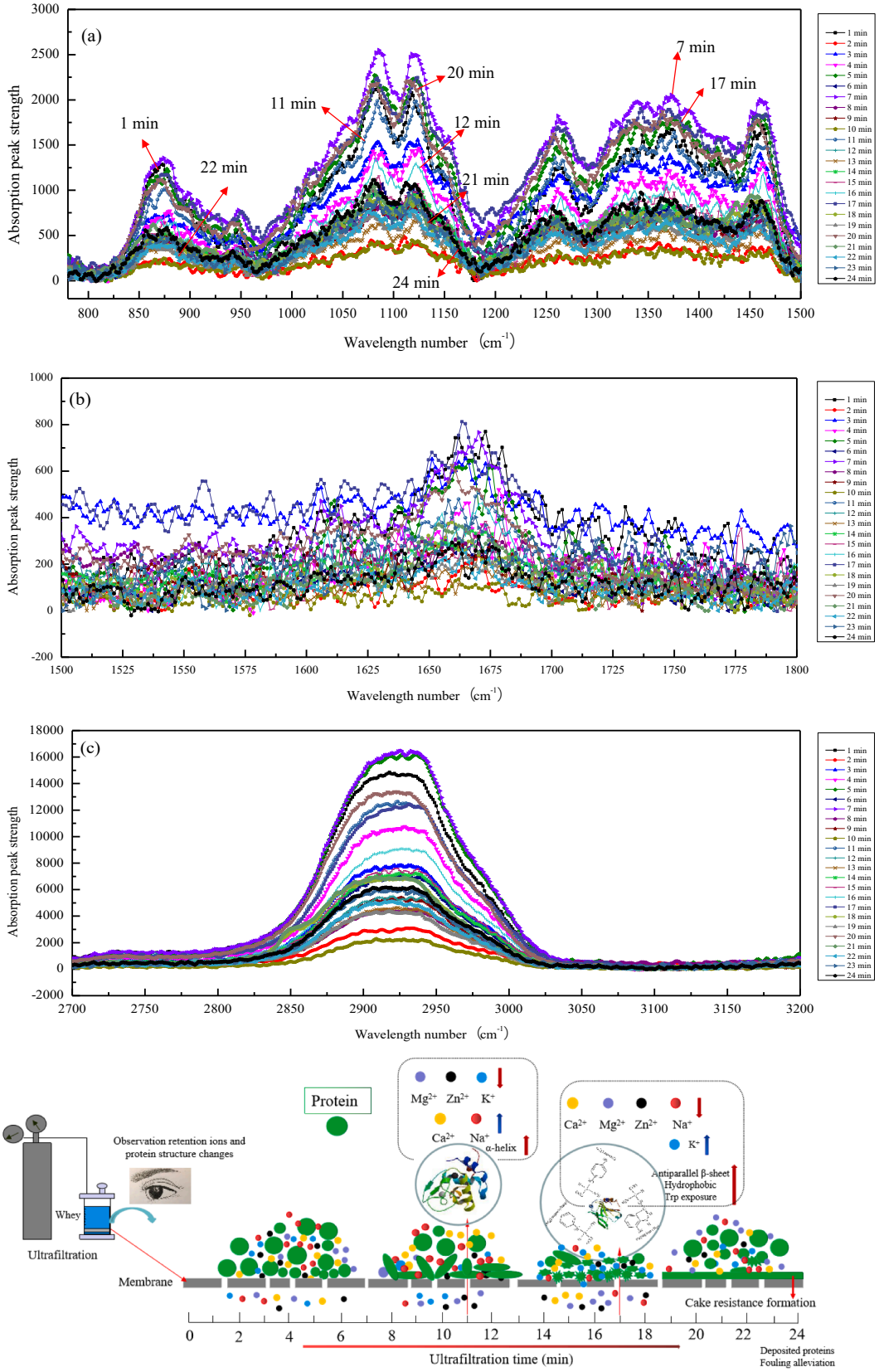

Fig. 5. Raman spectra (RS) of whey protein in retention during ultrafiltration process.

The secondary and surface structure changes of the retention protein during ultrafiltration

The changes in protein surface structure directly affect the changes in surface functional groups and then affect the interaction between proteins and proteins and between proteins and membranes. During the process of ultrafiltration, the change in protein secondary structure is not only related to the extension of ultrafiltration time but is also closely related to the ionic environment in solution. Salt ions can change the conformation of a protein or act as a salt bridge between the membrane and the protein, making it easier to precipitate (Hou, Lin, Zhao, Wang, & Fu, 2017). As shown in Fig. 4(a), the secondary structure of the whey protein changed in retention during filtration. The content of α-helix increased after 12 min, which was related to the intermolecular or intramolecular hydrogen bonds of O—H at 3500–3300 cm^{-1} and 3500–3100 cm^{-1} of amide bonds decreasing before 12 min as shown in Fig. 4(b). The –COOH and –NH bonds at 1740–1550 cm^{-1} also decreased. This indicated that the hydrophilic fragments were decreased and buried inside (Portugal, Crespo, & Lima, 2007). The content of β-sheets also increased after 15 min, which led to hydrophobic bond exposure and some protein aggregation and deposition on the membrane surface and a decrease in membrane flux, as shown in Fig. 1(f). Furthermore, the ion concentrations of K^+, Mg^{2+} and Zn^{2+} decreased at 15–18 min and the concentrations of Ca^{2+} and Na^+ increased, which increased the hydrophobic properties of the protein. When the ion ratio became balanced after 21 min, similar to the initial filtration process, the protein in the retention had more hydrophilic bands at 3500–3100 cm^{-1} and 950–960 cm^{-1} with exposure on the surface, as shown in Fig. 4 (b). This is why the protein surface tension was decreased, as shown in Fig. 3(a). As shown in Fig. 4(a), the random curl content increased at 23 min. At this time, the membrane flux and protein content decreased, but the ion concentration increased. The reason was that the hydrogen bond broke, the protein structure folded, and the β-sheet changed to a random curl. The protein structure became more disordered, leading to increased membrane fouling.

Raman characteristic bands of the retention protein during ultrafiltration

As shown in Fig. 5(a), the band at 850/830 cm^{-1} for tyrosine was decreased compared to the beginning of filtration. This indicated that the amide of tyrosine was buried inside the formed α-helix. The intensity of the band at approximately 940 cm^{-1} (C—C—N stretching, α-helix) was considered to be proportional to the α-helix content. The C—H symmetric bending band located at approximately 1395 cm^{-1} was found to have an intensity that decreased as the protein α-helical content increased (Blanpain-Avet et al., 2012).

A higher band intensity at approximately 2930–2933 cm^{-1} was observed in the spectra of whey protein during filtration, reflecting more C—H stretching of aromatic and aliphatic amino acids, as shown in Fig. 5(c) (Wang, He, Labuza, & Ismail, 2013). However, the intensity of C—H stretching for aromatic and aliphatic amino acids was lower than at 1 min except for at 5 min and 7 min. The intensity at approximately 2930–2933 cm^{-1} decreased significantly, which indicated that the aromatic and aliphatic amino acids were buried inside or caused by protein aggregation and occlusion. At 12 min, the ions of Ca^{2+}, Na^+, Mg^{2+} and Zn^{2+} were completely decreased, and K^+ was increased, which indicated that the ratio of K^+ may lead to more aromatic and aliphatic amino acids buried inside and forming α-helices. Most of the protein particle sizes began to increase at 12 min, as shown in Fig. 2 (a). The intensity of 1400–1430 cm^{-1} attributed to aspartic acid and glutamic acid also decreased at 12 min. Therefore, the relatively higher K^+ retention could lead to more protein aggregation. Furthermore, the band representing the β-sheet configuration in the amide III region, which is often reported near 1230–1243 cm^{-1}, was decreased, which was similar to the CD results shown in Fig. 3(a). The band intensity at 1668 cm^{-1}, which corresponds to the antiparallel β-sheet configuration, increased significantly at 17 min. Furthermore, the intensity of the tryptophan band at 1360 cm^{-1} and the vibration of amide I (1655 cm^{-1}) were also increased, which means that some protein unfolding occurred. At this time, Ca^{2+}, Na^+, Mg^{2+} and Zn^{2+} also slightly decreased and K^+ increased. This also indicated that relatively higher K^+ retention could induce protein aggregation and accelerate membrane fouling. Ca^{2+}, Na^+, Mg^{2+} and Zn^{2+} had a tendency to increase at 21 min as shown in Fig. 1.The protein surface tension was decreased as shown in Fig. 3(a).

Conclusion

This study analyzed the retention protein structural changes caused by ion environment changes during the ultrafiltration process. From this point of view, the membrane fouling mechanism of whey protein ultrafiltration was revealed. The ion concentration and ratio had a considerable effect on whey protein surface tension and group exposure, which determine the hydrophilic and hydrophobic properties of proteins. This was very important for the time of membrane fouling formation during filtration. Ca^{2+} and Na^+ were overall increased, and other ion concentrations decreased, which increased the hydrophobic properties of the protein. The relatively higher K^+ retention could lead to an antiparallel β-sheet configuration, and aspartic acid, glutamic acid and tryptophan increased significantly, which increased protein aggregation and deposition on the membrane surface. When the ion concentration and ratio restored the balance and were close to the initial state, the protein surface tension was decreased, and the hydrophilic ability increased at 21–24 min. In this study, we were able to monitor the membrane fouling process and observe the ion ratio and concentration at a specific filtration time to analyze membrane fouling formation. Therefore, finding the best time to adjust the proportion of each ion and maintain the balance of the ionic environment in solution will be the key to optimizing the process. With the renewal of membrane technology and the combined use of various membrane processes, it is more efficient and convenient to concentrate protein using this technology. Although it has been implemented in commercial processes, the small-scale experimental research for new membrane materials and ions regulation methods showed that the recovery rate, purification rate and product quality have been steadily improved. Looking to the future, continuously optimized membrane technology will play an important role in the next generation of biotechnology.

CRediT authorship contribution statement

Wen-qiong Wang: Investigation, Formal analysis, Writing – original draft. **Jian-ju Li:** Methodology, Resources, Formal analysis. **Ji-yang Zhou:** Methodology, Resources. **Man-xi Song:** Data curation. **Jia-cheng Wang:** Investigation. **Xing Li:** Formal analysis. **Cong-Cong Tang:** Formal analysis. **Mao-lin Lu:** Supervision. **Rui-xia Gu:** Supervision, Funding acquisition.

Declaration of Competing Interest

The authors declare that they have no known competing financial interests or personal relationships that could have appeared to influence the work reported in this paper.

Acknowledgements

This work was supported by project of the National Science Foundation for Young Scientists of China (Grant No. 31901715). Jiangsu postdoctoral Foundation (2021K317C). Jiangsu provincial practice and innovation plan project (SJCX21_1630). Project funded by China Postdoctoral Science Foundation (2022M712433).

References

Adhikari, B., Howes, T., Shrestha, A., & Bhandari, B. R. (2007). Effect of surface tension and viscosity on the surface stickiness of carbohydrate and protein solutions. *Journal of Food Engineering, 79*(4), 1136–1143.

Ahn, W.-Y., Kalinichev, A. G., & Clark, M. M. (2008). Effects of background cations on the fouling of polyethersulfone membranes by natural organic matter: Experimental and molecular modeling study. *Journal of Membrane Science, 309*(1), 128–140.

Blanpain-Avet, P., Hédoux, A., Guinet, Y., Paccou, L., Petit, J., Six, T., & Delaplace, G. (2012). Analysis by Raman spectroscopy of the conformational structure of whey proteins constituting fouling deposits during the processing in a heat exchanger. *Journal of Food Engineering, 110*(1), 86–94.

Damar Huner, I., & Gulec, H. A. (2017). Fouling behavior of poly(ether)sulfone ultrafiltration membrane during concentration of whey proteins: Effect of hydrophilic modification using atmospheric pressure argon jet plasma. *Colloids and Surfaces B: Biointerfaces, 160*, 510–519.

Dineshbhai, C. K., Basaiawmoit, B., Sakure, A. A., Maurya, R., Bishnoi, M., Kondepudi, K. K., … Hati, S. (2022). Exploring the potential of Lactobacillus and Saccharomyces for biofunctionalities and the release of bioactive peptides from whey protein fermentate. *Food Bioscience, 101758*.

Ding, Y., Ma, B., Liu, H., & Qu, J. (2019). Effects of protein properties on ultrafiltration membrane fouling performance in water treatment. *Journal of Environmental Sciences, 77*, 273–281.

Gao, F., Wang, J., Zhang, H., Jia, H., Cui, Z., & Yang, G. (2018). Role of ionic strength on protein fouling during ultrafiltration by synchronized UV–vis spectroscopy and electrochemical impedance spectroscopy. *Journal of Membrane Science, 563*, 592–601.

Hou, D., Lin, D., Zhao, C., Wang, J., & Fu, C. (2017). Control of protein (BSA) fouling by ultrasonic irradiation during membrane distillation process. *Separation and Purification Technology, 175*, 287–297.

Kilmer, N. T., Huss, R. L., George, C. C., & Stennett, E. M. S. (2021). The influence of ion identity and ionic strength on membrane biofouling of a binary protein solution. *Separation and Purification Technology, 255*, Article 117769.

Klost, M., Giménez-Ribes, G., & Drusch, S. (2020). Enzymatic hydrolysis of pea protein: Interactions and protein fractions involved in fermentation induced gels and their influence on rheological properties. *Food Hydrocolloids, 105*, Article 105793.

Miao, R., Li, X., Wu, Y., Wang, P., Wang, L., Wu, G., … Liu, T. (2017). A comparison of the roles of Ca^{2+} and Mg^{2+} on membrane fouling with humic acid: Are there any differences or similarities? *Journal of Membranes, 545*, 81–87.

Miller, D. J., Kasemset, S., Wang, L., Paul, D. R., & Freeman, B. D. (2014). Constant flux crossflow filtration evaluation of surface-modified fouling-resistant membranes. *Journal of Membrane Science, 452*, 171–183.

Moghaddam, S. Z., & Hormann, E. T. (2019). The Hofmeister series: Specific ion effects in aqueous polymer solutions. *Journal of Colloid and Interface Science, 555*, 615–635.

Portugal, C., Crespo, J. G., & Lima, J. C. (2007). Monitoring the structural alterations induced in β-lactoglobulin during ultrafiltration: Learning from chemical and thermal denaturation phenomena. *Journal of Membrane Science, 300*(1–2), 211–223.

Portugal, C., Lima, J., & Crespo, J. (2006). Probing the change of enzymatic activity of horseradish peroxidase induced by membrane permeation using tryptophan fluorescence. *Journal of Membrane Science, 284*(1–2), 180–192.

Portugal, C. A. M., Lima, J. C., & Crespo, J. G. (2008). Effect of physicochemical conditions on the ultrafiltration of β-lactoglobulin: Fluorescence probing of induced structural changes. *Journal of Membrane Science, 321*(1), 69–80.

Rohani, M. M., & Zydney, A. L. (2010). Role of electrostatic interactions during protein ultrafiltration. *Advances in Colloid & Interface Science, 160*(1–2), 40–48.

Rui, M., Wang, L., Mi, N., Zhe, G., Liu, T., Lv, Y., … Yang, Y. (2015). Enhancement and Mitigation Mechanisms of Protein Fouling of Ultrafiltration Membranes under Different Ionic Strengths. *Environmental Science & Technology, 49*(11), 6574–6580.

Salgın, S., Takaç, S., & Özdamar, T. H. (2006). Adsorption of bovine serum albumin on polyether sulfone ultrafiltration membranes: Determination of interfacial interaction energy and effective diffusion coefficient. *Journal of Membrane Science, 278*(1), 251–260.

Sethuraman, A., & Belfort, G. (2005). Protein Structural Perturbation and Aggregation on Homogeneous Surfaces. *Biophysical Journal, 88*(2), 1322–1333.

She, Q., Tang, C. Y., Wang, Y.-N., & Zhang, Z. (2009). The role of hydrodynamic conditions and solution chemistry on protein fouling during ultrafiltration. *Desalination, 249*(3), 1079–1087.

Tang, C.-C., Zhang, X.-Y., Wang, R., Wang, T.-Y., He, Z.-W., & Wang, X. C. (2022). Calcium ions-effect on performance, growth and extracellular nature of microalgal-bacterial symbiosis system treating wastewater. *Environmental Research, 207*, Article 112228.

Van Audenhaege, M., Pezennec, S., & Gesan-Guiziou, G. (2013). Ultrafiltration membrane cut-off impacts structure and functional properties of transmitted proteins: Case study of the metalloprotein α-lactalbumin. *Separation and Purification Technology, 114*, 73–82.

Wagner, J., Biliaderis, C. G., & Moschakis, T. (2020). Whey proteins: Musings on denaturation, aggregate formation and gelation. *Critical Reviews in Food Science and Nutrition, 60*(22), 3793–3806.

Wang, Q., He, L., Labuza, T. P., & Ismail, B. (2013). Structural characterisation of partially glycosylated whey protein as influenced by pH and heat using surface-enhanced Raman spectroscopy. *Food Chemistry, 139*(1), 313–319.

Wang, Y. N., & Tang, C. Y. (2011). Fouling of nanofiltration, reverse osmosis, and ultrafiltration membranes by protein mixtures: The role of inter-foulant-species interaction. *Environmental Science & Technology, 45*(15), 6373–6379.

Wen-qiong, W., Lan-wei, Z., Xue, H., & Yi, L. (2017). Cheese whey protein recovery by ultrafiltration through transglutaminase (TG) catalysis whey protein cross-linking. *Food Chemistry, 215*, 31–40.

Wojciechowski, K. (2022). Surface tension of native and modified plant seed proteins. *Advances in Colloid and Interface Science, 302*, Article 102641.

Zhang, C., Bao, Q., Wu, H., Shao, M., Wang, X., & Xu, Q. (2022). Impact of polysaccharide and protein interactions on membrane fouling: Particle deposition and layer formation. *Chemosphere, 296*, Article 134056.

Zhao, J., Yang, Y., Li, C., Liang, J., & Hou, L. A. (2019). Impacts of mono/divalent cations on the lamellar structure of cross-linked GO layers and membrane filtration performance for different DOM fractions. *Chemosphere, 237*, Article 124544.